Journal of Luminescence 192 (2017) 218–223

Contents lists available at ScienceDirect

Journal of Luminescence

journal homepage: www.elsevier.com/locate/jlumin

Crystal structure characterization and up-conversion luminescent properties of $BaIn_2O_4$ phosphor

Shusen Chen[a], Wenjiang Wang[a], Keli Wang[a], Ming Guan[a], Maxim S. Molokeev[b,c], Lefu Mei[a,*], Zhaohui Huang[a,*]

[a] School of Materials Science and Technology, Beijing Key Laboratory of Materials Utilization of Nonmetallic Minerals and Solid Wastes, National Laboratory of Mineral Materials, China University of Geosciences, Beijing 100083, China
[b] Laboratory of Crystal Physics, Kirensky Institute of Physics, SB RAS, Krasnoyarsk 660036, Russia
[c] Department of Physics, Far Eastern State Transport University, Khabarovsk 680021, Russia

ARTICLE INFO

Keywords:
Crystal structure
Up-conversion
$BaIn_2O_4$

ABSTRACT

Er^{3+} / Yb^{3+} doped $BaIn_2O_4$ up-conversion (UC) phosphors are synthesized and their UC luminescent properties are characterized. $BaIn_2O_4$ has *P*21/*c* space group but Rietveld refinement suggests it has twice smaller cell parameter (a = 10.3975 Å, *b* = 5.8295 Å, *c* = 14.4457 Å) and volume than previous reported structure. Refinement also reveals Er^{3+}/Yb^{3+} replaces In^{3+} ions in lattice because of the existence of InO_6 octahedra. In these $BaIn_2O_4$ phosphors, co-doping with Yb^{3+} ions changes the predominant UC emission from green ($^2H_{11/2}$, $^4S_{3/2}$ → $^4I_{15/2}$ of Er^{3+}) to red (about 665 nm, $^4F_{9/2}$ → $^4I_{15/2}$ of Er^{3+}). By controlling of Er^{3+}/Yb^{3+} concentrations, the $BaIn_2O_4$ phosphors have the potential of generating various UC spectra and color tunability. The pumping powers study shows two-photon process in these phosphors.

1. Introduction

Up-conversion (UC) phosphors have drawn lots of attentions recently due to their significant potential applications in light emitting displays, solid state lighting and biological labeling [1–3]. As spectral modification materials, UC phosphors show importance for converting photons with low energy to those of high energy by "merging" low energy photons [4–6]. Though fluoride-based compounds are considered as the most excellent UC phosphors due to their low phonon energy, oxide-based UC phosphors which have relative low phonon energy such as Y_2O_3 and Gd_2O_3 also are widely studied [7,8]. Nowadays highly efficient oxide UC phosphors are still demanded because they not only show good UC luminescent properties but also exhibit high chemical stability. Moreover, they always are easy to synthesize. Alkaline earth ions (Ca^{2+}, Sr^{2+}, and Ba^{2+}) have close ionic radius to lanthanide ions, inorganic compounds containing these ions are frequently used as UC host materials [9–11].

Kalinina et al. [12] established the phase diagram for BaO-In_2O_3 system previously, however the structure of $BaIn_2O_4$ still have some mysteries [12,13]. As a oxide compound, $BaIn_2O_4$ has good mechanical durability, chemical and thermal properties. As a semiconducting compound, $BaIn_2O_4$ demonstrates large potential as UC oxide-based host. Previous reports showed the possible space group of *P*21/*a* (ICSD #202986) for $BaIn_2O_4$ [14–16], means the crystallographic sites of In^{3+} ions in distorted InO_6 octahedra can be substituted by lanthanide ions such as Er^{3+} and Yb^{3+} [17–19]. As well known, Er^{3+} is important UC active ions which can emit green or red light [20–22], and Yb^{3+} is good sensitive ions due to its strong absorption in the near-infrared light region [23,24]. Therefor whether Er^{3+} and Yb^{3+} ions doped $BaIn_2O_4$ UC phosphors have low phonon energy and good UC luminescent properties is deserved to study. In this work, green and red emitting Er^{3+}/Yb^{3+} doped $BaIn_2O_4$ phosphors were synthesized. Crystal structure characterization as well as UC luminescent properties of these Er^{3+}/Yb^{3+} doped $BaIn_2O_4$ were studied in detail. The findings contribute to the complement of indate-based and oxide-based UC phosphors system, more importantly, open the possibility of Er^{3+}/Yb^{3+} doped $BaIn_2O_4$ as novel phosphors which can generate various UC spectra and color tunability.

2. Experimental

2.1. Sample preparation

Samples were prepared via solid-state reaction method. In a typical synthesis procedure, raw materials of $BaCO_3$(A.R.), In_2O_3(99.995%), Er_2O_3 (99.995%), Yb_2O_3(99.995%) were weighted according to

* Corresponding authors.
E-mail addresses: mlf@cugb.edu.cn (L. Mei), huang118@cugb.edu.cn (Z. Huang).

http://dx.doi.org/10.1016/j.jlumin.2017.06.034
Received 28 November 2016; Received in revised form 1 May 2017; Accepted 17 June 2017
Available online 19 June 2017

stoichiometric ratio, and then mixed and ground thoroughly in an agate mortar. After that, the mixtures were transferred into alumina crucibles and sintered in muffle furnaces with different temperatures (1100–1500 °C, see Fig. S1). After these samples were cooled down to room temperature naturally, the resulted phosphors were fully ground again for the following measurements.

2.2. Characterization

The X-ray powder diffractometer (D8 Advance, Bruker Corporation, Germany, with Cu-Kα and linear VANTEC detector, λ = 0.15406 nm, 40 kV, 100 mA) was used for examine the crystal structure. Rietveld refinement was performed by using TOPAS 4.2 program. Raman spectra were collected using Raman Microscope (Horiba Jobin Yvon). Excitation wavelength was 633 nm with actual power of 46.0 μW. The UC luminescent spectra of the phosphors were recorded on a spectrophotometer (F-4600, Hitachi high technologies corporation, Tokyo, Japan) with an external power-controllable 980 nm semiconductor laser (Beijing Viasho Technology Company, Beijing, China) as the excitation source. The diffuse reflection spectra were measured on a UV-VIS-NIR spectrophotometer (Shimadzu UV-3600, Japan) attached to an integral sphere. All the tests were accomplished at room temperature.

3. Results and discussion

3.1. Crystal structure characterizations

Powder XRD Rietveld refinement was adopted to clarify the structure mysteries of these $BaIn_2O_4$ UC phosphors. First of all, crystal structure $BaIn_2O_4$ was solved previously in $P21/a$ space group and it was further transformed into space group $P21/c$ to get standard settings [25]. This structure was used as starting model for present Rietveld refinement which ended at R_B = 3.72% (Fig. 1a,b). Final crystal structure was checked by PLATON and by the internet service of IUCr which showed that there is nonspacegroup translation $a/2$. Therefore programs strongly recommended to halve cell parameter a, and to use new crystal structure with the same space group $P21/c$. New refinement ended at lower R_B = 3.49% and accounts the same peaks on the pattern by using twice less number of peaks (Fig. 1c). Difference Rietveld plots of both model look very similar (Fig. 1a,c), but new suggested model has twice smaller cell parameter and volume (Fig. 1b,d), twice smaller number of refinement parameters and it can be concluded that new model is better. There are two Ba^{2+} ions, four In^{3+} ions and eight O^{2-} ions in asymmetric part of new unit cell and this structure was determined as $P21/c$ space group (a = 10.3975 Å, b = 5.8295 Å, c = 14.4457 Å). It is important to note that some very small peaks at ~ 22 2θ° cannot be fitted and this is because Renninger-effect leads to the appearance of some weak peaks due to multiple diffractions from different planes inside of crystal [26,27].

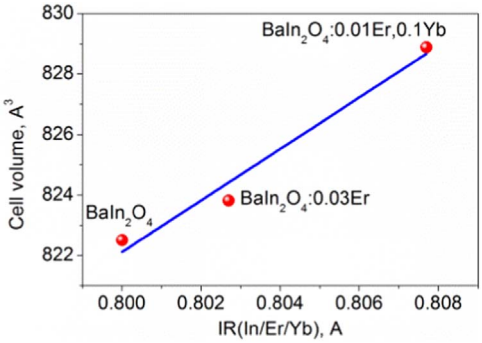

Fig. 2. Linear cell volume increasing per average ion radii IR(In/Er/Yb).

This solved model was used to make structure refinement of single Er^{3+} (0.03) doped and Er^{3+}/Yb^{3+} (0.01 / 0.1) co-doped $BaIn_2O_4$ phosphors. Linear increasing of cell volume per increasing concentration of doping elements (Fig. 2) proved the replacement of In^{3+} ions with small ion radii IR(In^{3+}, CN = 6) = 0.8 Å by bigger Er^{3+} and Yb^{3+} ions with IR(Er^{3+}, CN = 6) = 0.89 Å and IR(Yb^{3+}, CN = 6) = 0.868 Å, respectively. Therefore in models the sites of In^{3+} ion were occupied by random In^{3+} / Er^{3+} / Yb^{3+} ions with fixed occupations according to suggested chemical formulas (if Ba^{2+} were replaced, cell

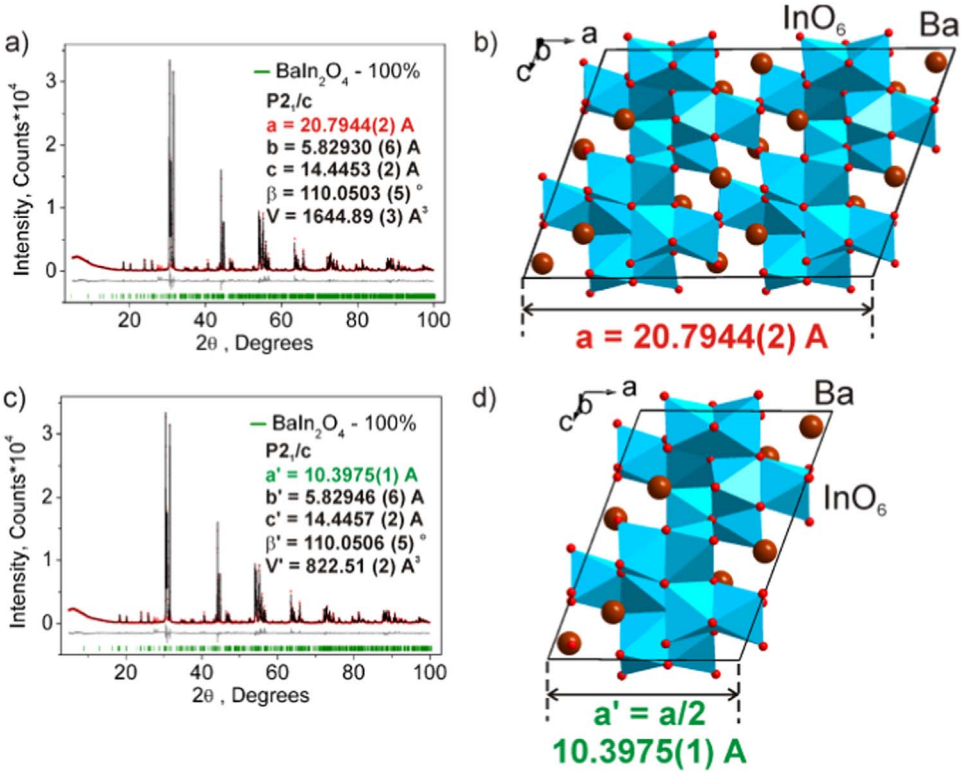

Fig. 1. XRD patterns and Rietveld plots of initial model (a) and new suggested model (c), and comparison initial crystal structure of $BaIn_2O_4$ (b) with new proposed structure (d).

Table 1
Main parameters of processing and refinement of the samples.

Compound	Phase	Sp.gr.	Cell parameters (Å, °), Volume (Å^3)	R_p, R_{wp} (%), χ^2	R_B (%)
$BaIn_2O_4$	$BaIn_2O_4$	$P2_1/c$	a = 10.3975 (1) b = 5.82946 (6) c = 14.4457 (2) β = 110.0506 (5) V = 822.51 (2)	7.06, 11.23, 2.78	3.49
$BaIn_2O_4$:0.03Er	$BaIn_2O_4$:0.03Er	$P2_1/c$	a = 10.4064 (2) b = 5.8319 (1) c = 14.4490 (3) β = 110.038 (1) V = 823.81 (3)	4.39, 6.67, 2.29	2.48
$BaIn_2O_4$:0.01Er, 0.1Yb	$BaIn_2O_4$:0.01Er, 0.1Yb	$P2_1/c$	a = 10.4357 (2) b = 5.84541 (8) c = 14.4654 (2) β = 110.0572 (6) V = 828.88 (2)	3.96, 6.70, 2.68	2.48

volume should decrease since Ba have bigger radii than Er^{3+} / Yb^{3+}). Refinements were stable and gave low R-factors (Table 1). Coordinates of atoms and main bond lengths also are shown in Table S1 and S2. Further details of the crystal structures can be obtained from FIZ Karlsruhe, 76344 Eggenstein-Leopoldshafen, Germany (deposition number CSD-433000–433002).

3.2. UC luminescent properties

Fig. 3 displays the UC spectrum of prepared $BaIn_2O_4$: xEr^{3+} / $0.1Yb^{3+}$ (x = 0.005, 0.007, 0.01, 0.03, 0.05, 0.07) phosphors upon 980 nm laser excitation. Non-doped $BaIn_2O_4$ and single Er^{3+}(0.03) doped $BaIn_2O_4$ also are shown. It is clear that the main emission peaks are centered at 665 nm (red light) in these Er^{3+} / Yb^{3+} co-doped samples, which are assigned to the $^4F_{9/2} \rightarrow {}^4I_{15/2}$ transitions of Er^{3+} ions [9,28]. Green emissions around 555 nm are weak but still can be observed from these spectra, and these emissions are attributed to $^2H_{11/2}$ ($^4S_{3/2}$) $\rightarrow {}^4I_{15/2}$ of Er^{3+}. No UC emissions can be observed in pure $BaIn_2O_4$ sample. Single Er^{3+} doped $BaIn_2O_4$ shows very weak UC emissions because of the absence of Yb^{3+} sensitizer, indicating the adding of Yb^{3+} ions greatly facilitate the UC emissions of $BaIn_2O_4$ phosphors. Because of concentration quench of Er^{3+}, UC emission intensity increases firstly, arrives maximum when Er^{3+} was determined as 0.03, and then decreases with the increasing Er^{3+} content (see inset). When Er^{3+} concentration is fixed as 0.03 and then change Yb^{3+} concentration, the optimal Yb^{3+} concentration is determined as 0.1, as seen in Fig. S2.

Interestingly, we observe the emissions of single Er^{3+} doped $BaIn_2O_4$ samples are close to green light region (555 nm and 665 nm comprise of the UC emission patterns). On the other hand, the emissions of Er^{3+} / Yb^{3+} co-doped $BaIn_2O_4$ sample are mainly concentrated at red light region (emission of 665 nm is predominant). Fig. 4 shows the comparison of UC emissions between single Er^{3+} doped and Er^{3+} / Yb^{3+} co-doped $BaIn_2O_4$ samples.

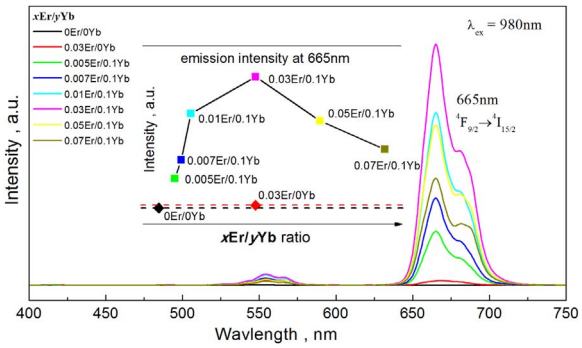

Fig. 3. UC spectra of pure, single Er^{3+} doped, and Er^{3+}/Yb^{3+} co-doped $BaIn_2O_4$: xEr^{3+} / $0.1Yb^{3+}$ (x = .005, 0.007, 0.01, 0.03, 0.05, 0.07) phosphors, the inset shows variation of emission intensities upon 665 nm. (For interpretation of the references to color in this figure legend, the reader is referred to the web version of this article.)

To study the reason why these phosphors show two different kinds of emissions, absorbance spectrum (Fig. 5a) and Raman spectrum (Fig. 5b) of pure $BaIn_2O_4$, single Er^{3+} doped $BaIn_2O_4$, single Yb^{3+} doped and $0.03Er^{3+}$ / $0.1Yb^{3+}$ co-doped $BaIn_2O_4$ samples are detected and analyzed. From Fig. 5a, Er^{3+} / Yb^{3+} co-doped sample shows obvious absorption band at 900 and 980 nm, which is $^2F_{7/2} \rightarrow {}^2F_{5/2}$ absorption of Yb^{3+} ions. Absorption band around 520, 650 and 800 nm are detected in both of single Er^{3+} doped and Er^{3+} / Yb^{3+} co-doped samples, which can be assigned to the ground absorption of Er^{3+}. Therefore intensive UC emissions of Er^{3+} / Yb^{3+} co-doped $BaIn_2O_4$ should originate from energy transfer from Yb^{3+} to Er^{3+}. From Fig. 5b, pure $BaIn_2O_4$ has its maximum phonon energy of 675 cm^{-1}, indicating $BaIn_2O_4$ has potential to be an excellent UC host because it just slight higher than the maximum phonon energy (~ 600 cm^{-1}) of the typical and efficient oxide host of Y_2O_3. The doped Er^{3+} ions do not change the maximum phonon energy in synthesized Er^{3+} doped $BaIn_2O_4$ phosphor. However, the maximum phonon energy increase to 1090 cm^{-1} in Yb^{3+} single doped and $0.03Er^{3+}$ / $0.1Yb^{3+}$ co-doped $BaIn_2O_4$ phosphor. It should be the large phonon energy of Er^{3+}/Yb^{3+} co-doped $BaIn_2O_4$ that resulted in the predominant red emissions. Anyway, Er^{3+} / Yb^{3+} doped $BaIn_2O_4$ shows excellent UC luminescent properties though it has higher phonon energy.

The presence of UC lifetimes is essential evidence to know the inner UC energy transfer process as well as the reason why Er^{3+} / Yb^{3+} co-doped samples show predominant red emissions. Fig. 6a–f demonstrate the UC decay curves and calculated lifetimes of Er^{3+} $^2H_{11/2}$ ($^4S_{3/2}$) $\rightarrow {}^4I_{15/2}$ (555 nm green emissions) and $^4F_{9/2} \rightarrow {}^4I_{15/2}$ (665 nm red emissions) transitions under 980 nm excitation for these Er^{3+} single doped and Er^{3+} / Yb^{3+} co-doped $BaIn_2O_4$ samples. Each decay curve is fitted into a mono-exponential function to extract the lifetime value (Fig. 6c, f). For the single Er^{3+} doped samples, lifetimes of both green emissions and red emissions fluctuate, and did not show regular with a rise Er^{3+} concentration from 0.01 to 0.2 (Fig. 6a, b, c). Specifically, the lifetimes of typical $0.03Er^{3+}$ doped sample are determined as τ(555 nm) = 45.8 μs and τ(665 nm) = 28.5μs. After that, when Er^{3+} concentration was fixed as 0.03 in the Er^{3+} / Yb^{3+} co-doped $BaIn_2O_4$, it is easy to see the lifetimes of either green emissions or red emission decrease obviously with the increasing Yb^{3+} concentration (Fig. 6e, f, g). The lifetimes of τ(555 nm) = 51.4 μs and τ(665 nm) = 40 μs of typical $0.03Er^{3+}$ / $0.01Yb^{3+}$ doped sample are longer than those of single $0.03Er^{3+}$ doped sample, testifying the presence of Yb^{3+} facilitated UC

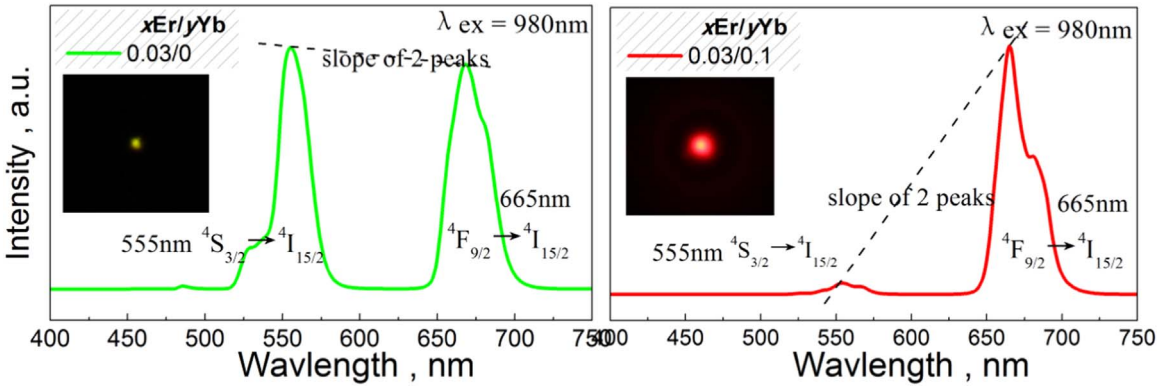

Fig. 4. Comparison of UC luminescent spectra between single Er^{3+} doped and Er^{3+}/Yb^{3+} co-doped $BaIn_2O_4$ phosphor. (For interpretation of the references to color in this figure legend, the reader is referred to the web version of this article.)

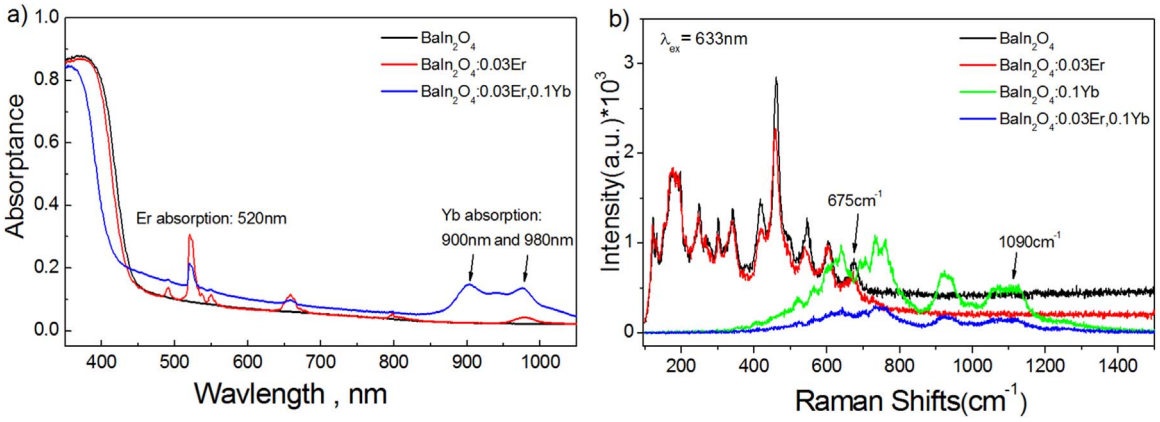

Fig. 5. Absorbance spectrum (a) and Raman spectrum (b) of pure $BaIn_2O_4$, single $0.03Er^{3+}$ doped $BaIn_2O_4$, single $0.1Yb^{3+}$ doped $BaIn_2O_4$ and $0.03Er^{3+}$ / $0.1Yb^{3+}$ co-doped $BaIn_2O_4$. (For interpretation of the references to color in this figure legend, the reader is referred to the web version of this article.)

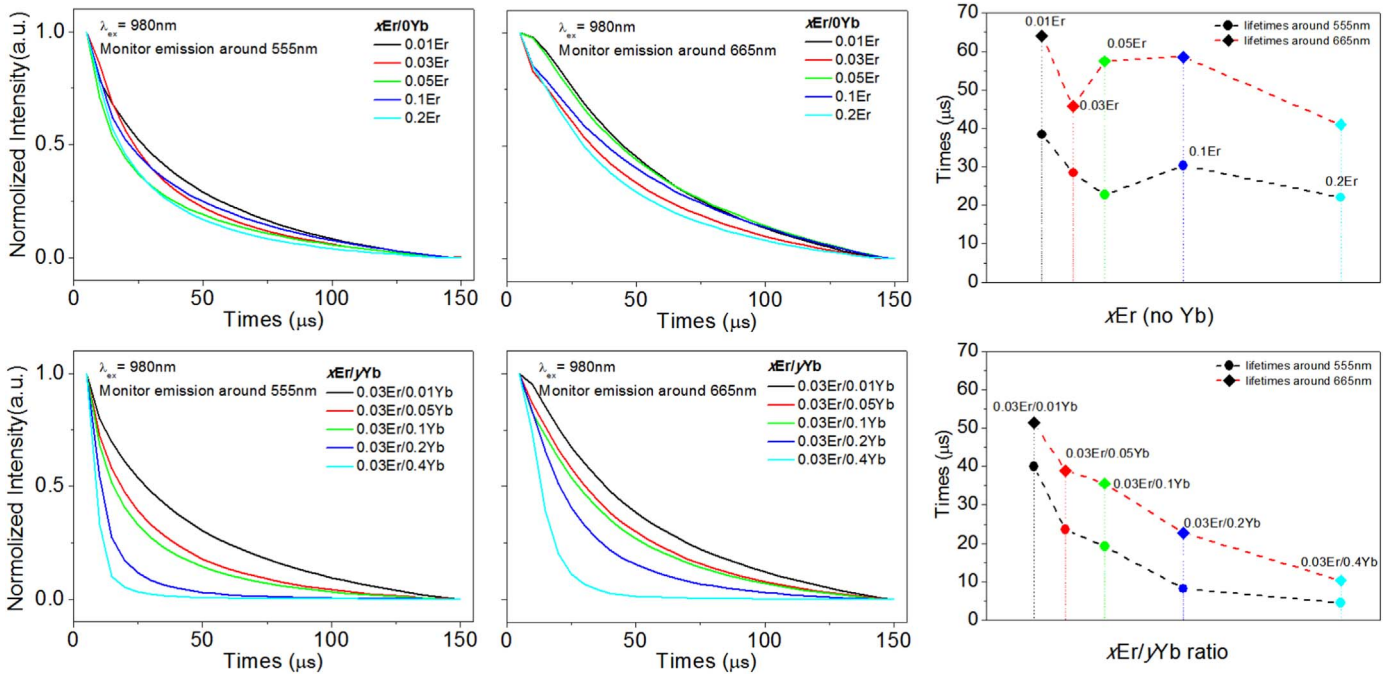

Fig. 6. UC decays of different Er^{3+} concentration doped $BaIn_2O_4$: xEr^{3+} (x = 0.01, 0.03, 0.05, 0.1, 0.2) samples under monitoring 555 nm red emissions (a), 665 nm green emissions (b), and calculated effective lifetimes (c); UC decays of different $0.03Er^{3+}$ / yYb^{3+} concentration co-doped $BaIn_2O_4$: $0.03Er^{3+}$ / yYb^{3+} (y = 0.01, 0.05, 0.1, 0.2, 0.4) samples under monitoring 555 nm red emissions (d), 665 nm green emissions (e), and calculated effective lifetimes (f). (For interpretation of the references to color in this figure legend, the reader is referred to the web version of this article.)

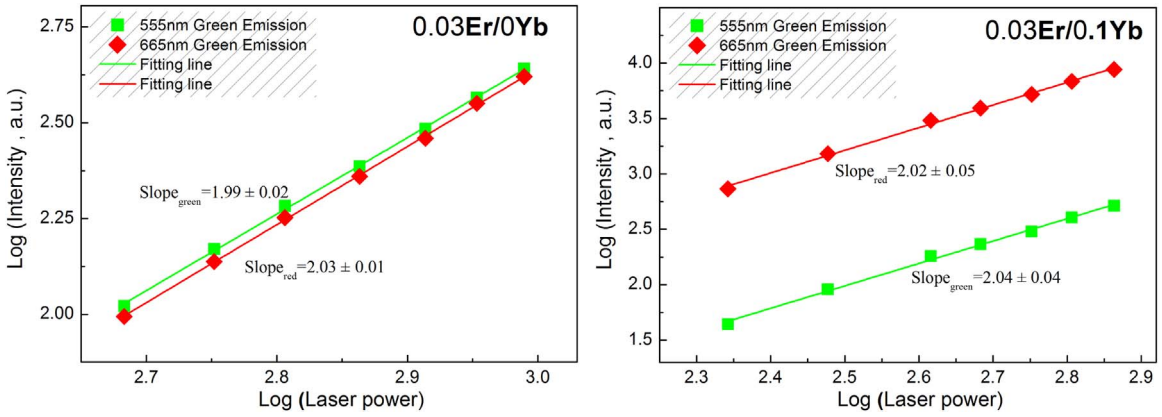

Fig. 7. Dependence of green and red UC emission intensities upon pumping power for single Er^{3+} doped and Er^{3+}/Yb^{3+} co-doped $BaIn_2O_4$ phosphor. (For interpretation of the references to color in this figure legend, the reader is referred to the web version of this article.)

emissions of Er^{3+} active ions. On the other hand, decreased lifetimes with a rise Yb^{3+} concentration (from 0.01 to 0.4) indicate back energy transfer processes are participated from the Er^{3+} activators to Yb^{3+} sensitizers in these Er^{3+}/Yb^{3+} co-doped $BaIn_2O_4$ samples. Because lifetime of Er^{3+} $^2H_{11/2}$ ($^4S_{3/2}$) → $^4I_{15/2}$ transition (555 nm green emissions) decrease more faster than that of $^4F_{9/2}$ → $^4I_{15/2}$ transition (555 nm emission dot line has larger slope in Fig. 6f), more energy on $^2H_{11/2}$ ($^4S_{3/2}$) instead of $^4F_{9/2}$ level of Er^{3+} is transferred back to Yb^{3+}, finally leading to a predominant red UC emission in Er^{3+}/Yb^{3+} co-doped $BaIn_2O_4$ samples.

Fig. 7 shows the dependence of green and red UC emission intensities upon pumping power for single Er^{3+} doped and Er^{3+}/Yb^{3+} co-doped $BaIn_2O_4$ phosphors. UC emission intensity (I_{em}) depending on the pumping laser power (P_{pump}) follows the relation of $I_{em} \propto (P_{pump})^n$, where n (slope of log I_{em} versus log P_{pump}) is the required number of pump photons for the transition from ground state to the upper emitting state [29]. In single Er^{3+} doped $BaIn_2O_4$ sample, the calculated slopes were 2.03 ± 0.01 for the red emission and 1.99 ± 0.02 for the green emission. In Er^{3+}/Yb^{3+} co-doped $BaIn_2O_4$ phosphor, the slopes were determined as 2.02 ± 0.05 for the red and 2.04 ± 0.04 for the green emission. Accordingly, the UC luminescent process in the novel Er^{3+} or/and Yb^{3+} doped $BaIn_2O_4$ phosphors is two-photon process.

4. Conclusions

Er^{3+}/Yb^{3+} doped $BaIn_2O_4$ phosphors are synthesized at 1400 °C by a solid-state reaction method. In this work, Rietveld refinement is employed to characterize the crystal structure, and it shows $BaIn_2O_4$ belongs to the space group of $P21/c$ and has twice smaller cell parameter and volume (a = 10.3975 Å, b = 5.82946 Å, c = 14.4457 Å, V = 822.51 Å^3) than the previous reported structure. In^{3+} ions are replaced by bigger Er^{3+} and Yb^{3+} ions, leading to linear enlargement of cell volume with increasing rare-earth ions. In these Er^{3+}/Yb^{3+} doped $BaIn_2O_4$ phosphors, increasing Yb^{3+} ions concentration changed the predominant UC emission from green ($^2H_{11/2}$, $^4S_{3/2}$ → $^4I_{15/2}$ of Er^{3+}) to red (about 665 nm, $^4F_{9/2}$ → $^4I_{15/2}$ of Er^{3+}). This is attributed to Yb^{3+} changed maximum phonon energy, and then part energy on $^2H_{11/2}$ ($^4S_{3/2}$) instead of $^4F_{9/2}$ level of Er^{3+} is transferred to Yb^{3+} through back energy transfer processes. Anyway, Er^{3+}/Yb^{3+} doped $BaIn_2O_4$ present excellent UC luminescent properties, and these novel $BaIn_2O_4$ phosphors show great potential to generate various UC spectra and color tunability by controlling of Er^{3+} / Yb^{3+} concentrations.

Acknowledgements

This present work was supported by the National Natural Science Foundations of China (Grant No. 51202226), the Fundamental Research Funds for the Central Universities (Grant nos. 2652016051, 2652016037), and Science and Technology Innovation Fund of the China University of Geosciences (Beijing) (Grant no. 201511415021).

Appendix A. Supplementary material

Supplementary data associated with this article can be found in the online version at http://dx.doi.org/10.1016/j.jlumin.2017.06.034.

References

[1] S. Gai, P. Yang, C. Li, W. Wang, Y. Dai, N. Niu, J. Lin, Synthesis of magnetic, up-conversion luminescent, and mesoporous core-shell-structured nanocomposites as drug carriers, Adv. Funct. Mater. 20 (2010) 1166–1172.
[2] R. Martín-Rodríguez, A. Meijerink, Infrared to near-infrared and visible upconversion mechanisms in $LiYF_4$:Yb^{3+}, Ho^{3+}, J. Lumin. 147 (2014) 147–154.
[3] F. Wang, R. Deng, J. Wang, Q. Wang, Y. Han, H. Zhu, X. Chen, X. Liu, Tuning upconversion through energy migration in core-shell nanoparticles, Nat. Mater. 10 (2011) 968–973.
[4] S. Gai, C. Li, P. Yang, J. Lin, Recent progress in rare earth micro/nanocrystals: soft chemical synthesis, luminescent properties, and biomedical applications, Chem. Rev. 114 (2014) 2343–2389.
[5] Q. Zhang, B. Zhu, Y. Zhuang, G. Chen, X. Liu, G. Zhang, J. Qiu, D. Chen, Quantum cutting in Tm^{3+}/Yb^{3+}-codoped lanthanum aluminum germanate glasses, J. Am. Ceram. Soc. 93 (2010) 654–657.
[6] J. Zhou, G. Chen, E. Wu, G. Bi, B. Wu, Y. Teng, S. Zhou, J. Qiu, Ultrasensitive polarized up-conversion of Tm^{3+}-Yb^{3+} doped beta-$NaYF_4$ single nanorod, Nano Lett. 13 (2013) 2241–2246.
[7] J. Zhao, Z. Lu, Y. Yin, C. McRae, J.A. Piper, J.M. Dawes, D. Jin, E.M. Goldys, Upconversion luminescence with tunable lifetime in $NaYF_4$:Yb,Er nanocrystals: role of nanocrystal size, Nanoscale 5 (2013) 944–952.
[8] F. Wang, X. Liu, Recent advances in the chemistry of lanthanide-doped upconversion nanocrystals, Chem. Soc. Rev. 38 (2009) 976–989.
[9] D. Li, Y. Wang, X. Zhang, K. Yang, L. Liu, Y. Song, Optical temperature sensor through infrared excited blue upconversion emission in Tm^{3+} / Yb^{3+} codoped Y_2O_3, Opt. Commun. 285 (2012) 1925–1928.
[10] T. Li, C. Guo, Y. Wu, L. Li, J.H. Jeong, Green upconversion luminescence in Yb^{3+}/Er^{3+} co-doped $ALn(MoO_4)_2$ (A = Li, Na and K; Ln=La, Gd and Y), J. Alloy. Compd. 540 (2012) 107–112.
[11] L. Li, C. Guo, S. Jiang, D.K. Agrawal, T. Li, Green up-conversion luminescence of Yb^{3+}-Er^{3+} co-doped $CaLa_2ZnO_5$ for optically temperature sensing, RSC Adv. 4 (2014) 6391.
[12] T.A. Kalinina, L.N. Lykova, L.M. Kovba, M.G. Mel'nikova, N.V. Porotnikov, Phase diagrams of BaO-In_2O_3 system, Russ. J. Inorg. Chem. 28 (1983) 259–262.
[13] X. Fan, L.M. Su, G.M. Cai, H.S. Liu, Z.P. Jin, Experimental determination and hermodynamic calculation of BaO-In_2O_3-B_2O_3 system, CALPHAD: Comput. Coupling Phase Diagr. Thermochem. (2016), http://dx.doi.org/10.1016/j.calphad.2016.11.001.
[14] A.N. Bondarchuk, A.B. Glot, C. Leyva-Porras, J.A. Aguilar-Martinez, Current-limiting effect in barium-doped indium oxide ceramics, J. Electron. Mater. 44 (2015) 3646–3653.
[15] Z.Z. Junwang Tang, Jinhua Ye, Effects of substituting Sr^{2+} and Ba^{2+} for Ca^{2+} on the structural roperties and photocatalytic behaviors of $CaIn_2O_4$, Chem. Mater. 16 (2004) 1644–1749.
[16] P. Ren, L.C. Zhou, J.X. Zhang, H. Yun, Synthesis mechanism and microstructure characterization of $BaIn_2O_4$, Adv. Mater. Res. 347–353 (2011) 1342–1347.
[17] M. Guan, H. Zheng, L. Mei, M.S. Molokeev, J. Xie, T. Yang, X. Wu, S. Huang, Z. Huang, A. Setlur, Preparation, structure, and up-conversion luminescence of Yb^{3+}/Er^{3+} codoped $SrIn_2O_4$ phosphors, J. Am. Ceram. Soc. 98 (2015) 1182–1187.
[18] T. Li, C. Guo, L. Li, Up-conversion luminescence of Er^{3+}-Yb^{3+} co-doped $CaIn_2O_4$,

Opt. Express 21 (2013) 18281–18289.
[19] M. Guan, H. Zheng, L. Mei, Z. Huang, T. Yang, M. Fang, Y. Liu, Infrared-to-visible up-conversion luminescence and energy transfer of RE^{3+} / Yb^{3+}(RE = Ho, Tm) co-doped $SrIn_2O_4$, Infrared Phys. Technol. 67 (2014) 107–110.
[20] S. Fischer, R. Martín-Rodríguez, B. Fröhlich, K.W. Krämer, A. Meijerink, J.C. Goldschmidt, Upconversion quantum yield of Er^{3+}-doped β-$NaYF_4$ and Gd_2O_2S: the effects of host lattice, Er^{3+} doping, and excitation spectrum bandwidth, J. Lumin. 153 (2014) 281–287.
[21] R. Wang, X. Zhang, F. Liu, L. Xiao, Y. Chen, L. Liu, Upconversion mechanisms of Er^{3+}:$NaYF_4$ and thermal effects induced by incident photon on the green luminescence, J. Lumin. 175 (2016) 35–43.
[22] S. Das, A. Amarnath Reddy, S. Surendra Babu, G. Vijaya Prakash, Tunable visible upconversion emission in Er^{3+}/Yb^{3+}-codoped $KCaBO_3$ phosphors by introducing Ho^{3+} ions, Mater. Lett. 120 (2014) 232–235.
[23] Z. Xia, J. Li, Y. Luo, L. Liao, J. Varela, Comparative investigation of green and red upconversion luminescence in Er^{3+} Doped and Yb^{3+} / Er^{3+} Codoped LaOCl, J. Am. Ceram. Soc. 95 (2012) 3229–3234.
[24] C. Zhong, P. Yang, X. Li, C. Li, D. Wang, S. Gai, J. Lin, Monodisperse bifunctional Fe_3O_4@$NaGdF_4$:Yb/Er@$NaGdF_4$:Yb/Er core–shell nanoparticles, RSC Adv. 2 (2012) 3194.
[25] H. Muller-Buschbaum, A. Lalla, Zur Verbindungsbildung MeO: M_2O_3. XI die Kristallstruktur von $BaIn_2O_4$, J. Less-Common Met. 154 (1989) 233–241.
[26] A. Sazonov, M. Meven, G. Roth, R. Georgii, I. Kezsma rki, V. Kocsis, Y. Tokunaga, Y. Taguchi, Y. Tokura, V. Hutanu, Origin of forbidden reflections in multiferroic $Ba_2CoGe_2O_7$ by neutron diffraction: symmetry lowering or Renninger effect, J. Appl. Cryst. 49 (2016) 556–560.
[27] E. Rossmanith, Multiple diffraction in the kinematical approach, Acta Cryst. A62 (2006) 174–177.
[28] Y. Yang, C. Mi, F. Yu, X. Su, C. Guo, G. Li, J. Zhang, L. Liu, Y. Liu, X. Li, Optical thermometry based on the upconversion fluorescence from Yb^{3+} / Er^{3+} codoped La_2O_2S phosphor, Ceram. Int. 40 (2014) 9875–9880.
[29] M. Pollnau, D.R. Gamelin, S.R. Luthi, H.U. Gudel, Power dependence of upconversion luminescence in lanthanide and transition-metal-ion systems, Phys. Rev. B 61 (2000) 3337–3346.